



Electromagnetic scattering by refractive index variations over a rough conducting surface

Y. HATZIIOANNOU† and M. SPIVACK

Department of Applied Mathematics and Theoretical Physics, The University of Cambridge CB3 9EW, UK

(Received 23 March 1999; revision received 15 November 2000)

Abstract. This paper presents a numerical method for calculating the scattered field when a vertically polarized Gaussian beam is incident on a flat or slightly rough conducting surface at a grazing angle and the refractive index of the propagation medium has a profile which is not constant. The method is a solution to the parabolic approximation of the full wave equation. The results presented are taken for a linear and log-linear refractive index profile.

1. Introduction

This paper concludes the work which started with the presentation of the image medium method for the solution of the scattering problem when an electromagnetic wave meets a conducting surface and the reflection coefficient is a function of the angle of incidence [1]. In this second paper we introduce the effects of a refractive index which may vary with both range and height above the surface.

Electromagnetic waves propagating over sea or land undergo scattering by a rough conducting surface, combined with distortion by refractive index variations. Surface interaction at low grazing angles gives rise to high-order multiple scattering and has been the subject of many theoretical, computational, and experimental studies (e.g. [2-6]). When forward-scattering predominates a useful numerical simplification is the parabolic integral approximation [7, 8]. Much attention has also been given to propagation through irregular media, often by parabolic equation methods (e.g. [9-11]). Very few rough surface models, however, have taken account of refractive index variations, and almost none in the presence of finite conductivity; similarly the irregular medium models incorporate rough boundary conditions only by use of further approximations or hybrid methods.

An image method based on the parabolic wave equation was applied in [1] to finitely conducting rough surfaces, in the absence of refractive index variation.

This model is extended here to spatially-varying refractive index profiles, which represent ducting over a rough sea surface. In addition to a mean height-dependent profile, turbulence may give rise to further spatial fluctuations. The advantage of this marching method is that the irregular boundary is replaced by a modified refractive index so that further variations are incorporated naturally. Two mean profiles are considered here: linear, bending the beam away from the

† Current address: Pisiadis 19, New Smyrna 171 24, Athens, Greece.

surface, and log-linear, trapping part of the beam close to the surface. In this paper we restrict our attention to a vertically polarized incident field, which allows the reflection coefficient to vary considerably with the angle of incidence.

In section 2 we describe the linear and log-linear refractive index profiles, and in section 3 we summarize the image medium approach. The main results are presented in section 4, for a flat and a *Pierson-Moscoviz* sea surface. As in the previous treatment the incident wave has the form of a Gaussian beam, the problem can be considered to be two-dimensional, and the surfaces considered are rough.

2. Varying refractive index profile

The main aim of this paper is the inclusion of spatial variations of refractive index in modelling conductive surface scattering. One of the principle applications is to the atmosphere over the sea surface, where several ducting mechanisms occur. For illustrative purposes we focus attention on the *evaporation duct*, which is briefly described here, following [12]. Immediately above the sea surface the atmosphere is often saturated. The saturation decreases rapidly with height, the decay being initially logarithmic. This leads to refractive index variations which form an evaporation duct, with a log-linear dependence. This is a reasonable assumption confirmed by comparison with meteorological measurements [13]. The duct height varies from around 6 m in the North Sea to 10 or 15 m in the Mediterranean and tropical regions, depending on factors such as the season, location and wind speed.

The discussion here concerns the mean refractive index, which is treated as a function of height z only, with vanishing horizontal gradients. Note however that this is not a restriction of the numerical model, which as shown below can deal with arbitrary spatial fluctuations.

If n is the refractive index over a curved earth, it is common to introduce the modified refractive index

$$m = n + \frac{z}{r_0}, \quad (1)$$

where r_0 is the earth's radius. (The small additional term allows for the earth's curvature when using flat-earth models. It is introduced because in the troposphere n decreases with height and is therefore downward refracting, but this effect is insufficient to overcome the earth's curvature.) Ducting layers can then be identified as regions in which m has a negative vertical derivative. This quantity is used from now on in our calculations. A duct occurs when m decreases with height z and has a thickness z_d when

$$dm/dz \begin{cases} < 0, & \text{for } z < z_d, \\ = 0, & \text{for } z = z_d, \\ > 0, & \text{for } z > z_d. \end{cases} \quad (2)$$

One duct occurring over the sea surface is the evaporation duct. This has the effect of a duct bending an electromagnetic beam travelling close to the surface, and if strong enough traps it over the surface. These phenomena will be graphically shown below.

Using the *Debye formula* [14] for *refractivity*

$$N = 77.6 \frac{P}{T} + 3.73 \times 10^5 \frac{e}{T^2}, \quad (3)$$

we can see how temperature T and water vapour pressure e are two factors that affect the formation of an evaporation duct, where $N = 10^6(n - 1)$. In many regions the sea surface is warmer than the atmosphere, $T_0 > T_z$, and also $e_0 < e_z$ due to transport of moisture from the sea to the upper layers of the atmosphere because of turbulent and convective transfer mechanisms. In these cases an evaporation duct cannot occur. However, there are certain meteorological conditions that allow the creation of a duct. There are areas where the sea surface is cooler than the air flowing over it. This usually happens in coastal regions and especially along the west coast of continents where warm, dry air moves over colder water. Thus, meteorological conditions and geographical position are factors that affect duct formation. The thickness of the duct also varies from place to place. It is about 6 m at the North Sea and can reach 15 m at the tropical regions [12].

We now concentrate on producing a formula for the variation of m with respect to the height z . The potential refractive index n_p may be defined [12] as

$$n_p = n + \frac{z}{r_0} - \frac{c_1 z}{r_0} \equiv m - \frac{c_1 z}{r_0},$$

where the quantity c_1 is a function of air pressure P , temperature T , gravitational acceleration g , gas constant of dry air R and specific heat of air c_p . For small height intervals c_1 may be regarded as constant [12], and from measurements made at the North Sea, has a computed value of $1/c_1 = 1.205 \pm 0.001$. Differentiation of (3) with respect to z [12] then leads to a relation between the refractive index m and the potential refractive index n_p :

$$m - m_0 = c_1 \frac{z}{r_0} + n_p - n_{p_0}, \quad (4)$$

where 0 denotes surface values.

In equation (4) the variation of $n_p - n_{p_0}$ depends on the status of the atmospheric stability. In the case of a neutral atmosphere, which is of interest to us in this paper, this variation is logarithmic:

$$\frac{n_p - n_{p_0}}{n_{p_r} - n_{p_0}} = \frac{\ln\left(\frac{z + h_0}{h_0}\right)}{\ln\left(\frac{z_r + h_0}{h_0}\right)}, \quad (5)$$

where z_r is a reference height. The quantity h_0 (referred to in [12] as a roughness parameter of the atmospheric surface layer) has a measured value of 1.5×10^{-4} m [15].

Substituting (5) in (4) and using the fact that $(\partial m / \partial z)_{z_d} = 0$, m can be written in the form:

$$m = m_0 + \alpha z + \beta \ln[f(z)] \quad (6)$$

where $\alpha = c_1/r_0$, $\beta = -(c_1/r_0)(z_d + h_0)$, $f(z) = z + h_0/h_0$.

This is a log-linear variation of m with height z . For $z < z_d$ the logarithmic term dominates while for $z > z_d$ the linear term is dominant. Figure 1 presents this log-linear profile of the refractive index compared with a constant and a linear

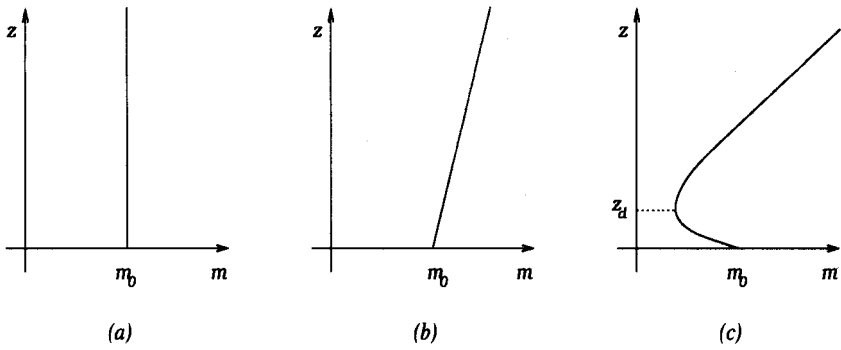


Figure 1. (a) Constant profile $m = m_0$. (b) Linear profile $m = m_0 + \alpha z$. (c) Log-linear profile $m = m_0 + \alpha z + \beta \ln[f(z)]$.

profile. This concludes our brief discussion on the refractive index variations. In the next section we incorporate it in the modified image medium method of [1]. In the last section we discuss the effects such variations have on the beam propagation using the results from the above combination.

3. The image medium method

This paper is concerned with a vertically polarized incident field, propagating through a varying refractive index and scattered by a rough conducting surface. We adapt the modified image medium method explained in [1] where it was applied to a rough surface. In order to incorporate a varying refractive index we must return to the formula given in [1] for the generalized refractive index N and substitute n using equation (6) with the appropriate coefficients α, β .

We briefly summarize the method and governing equations: the field is assumed to obey the parabolic wave equation, above a rough surface. The rough surface and lower half-space are then replaced by an image medium, with an image source, whose refractive index profile reflects the properties of the surface. After some algebraic manipulations [1] the following equation is derived:

$$\frac{\partial E}{\partial x} = \frac{i}{2\kappa_0} \frac{\partial^2 E}{\partial z^2} + \frac{i\kappa_0}{2} N(x, z) E, \tag{7}$$

where

$$E(x, z) = \begin{cases} E_R(x, z), & z > S(x), \\ E_I(x, z) \exp\{2i\kappa_0 S'(x)[z - S(x)]\}, & z < S(x), \end{cases} \tag{8}$$

and

$$N(x, z) = \begin{cases} n^2(x, z) - 1, & z > S(x), \\ n^2(x, -z + 2S(x)) - 1 + 4S''(x)[z - S(x)], & z < S(x). \end{cases} \tag{9}$$

Here E is the field, $S(x)$ denotes the surface and n is the refractive index. The functions E_R, E_I are the ‘real’ and ‘image’ solutions, and as in [1] it can be shown that this system obeys the required boundary conditions. This differential equation is then solved by a straightforward marching technique.

The procedure for the horizontally polarized incident field is identical. However, since the modified image medium method solves in a sense a more general problem we shall present the results of the vertical polarization case. (The results are qualitatively similar, except that the rough surface causes greater loss of energy into diffuse directions for vertical polarization, and the interference patterns, most evident for flat surfaces, are shifted.) This will be done in the next section.

4. Results

In this section we consider both a flat sea surface and a surface with a Pierson-Moscovitz spectrum (e.g. [16]) with wind speed $v = 15$ and present the results using two refractive index profiles. The spectrum takes the form:

$$\rho(\omega) = \frac{\alpha}{4|\omega|^3} \exp\left(-\frac{\beta g^2}{v^4 |\omega|^2}\right). \quad (10)$$

This form results from competing mechanisms of dissipation and wind generation. Unless stated otherwise the data used for the graphs are: *sea water conductivity*: $g = 4.3$; *sea water permittivity*: $\epsilon = 14.963 \times 10^{-12}$; *frequency*: $\varpi = 10^9$; *Gaussian beam centre*: $z_0 = 5$ m; *Gaussian beam half width*: $w = 0.5$ m; *horizontal range of propagation*: $x = 2000$ m; and *duct height*: $z_d = 15$ m. These data are the same as those used in [1] with the addition of the duct height and the increase of the propagation range to 2 km so that the duct effects are more obvious. The quantity presented in the graphs is the square root of the field intensity \mathcal{I} .

4.1. Linear profile

The profile considered here is of the form

$$m = m_0 + \alpha z, \quad (11)$$

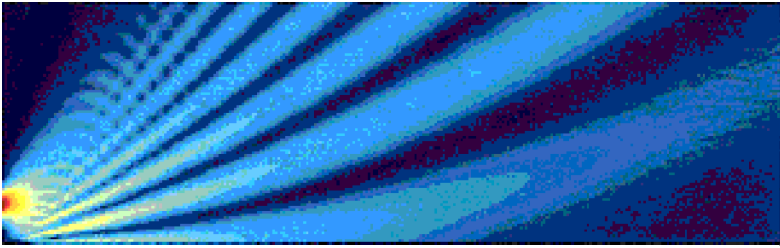
where $\alpha = c_1/r_0$ as in equation (6). The quantity α is always positive and so the refractive index is always increasing. As a result, the Gaussian beam bends away from the sea surface as is apparent in figure 2 (flat surface) and figure 3 (*Pierson-Moscovitz* surface). An obvious result of the upward refraction is that less energy impinges on the surface as the range increases, so that the bulk of the scattering arises from surface interaction near the source.

The value for the parameter $1/c_1$ given in the previous section results in a very small increase of the refractive index which is not very pronounced over this range of propagation, and we shall therefore present results for the value $1/c_1 = 0.01$ for which the effect is more clearly visible.

4.2. Log-linear profile

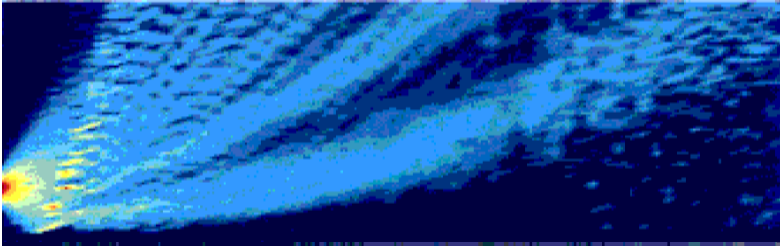
In this case we consider the profile form given in equation (6). The refractive index, as in figure 1(c), decreases logarithmically to a height $z = z_d$ and then increases linearly. This means that the part of the beam that enters the area $z < z_d$ bends towards the surface and a part of it becomes trapped in the duct. This effect can be seen in figure 4 (flat surface) and figure 5 (*Pierson-Moscovitz* surface).

The computed value of $1/c_1 = 1.205 \pm 0.001$ from measurements made in the *German Bight* again gives an extremely weak duct (figure 6) and has relatively little



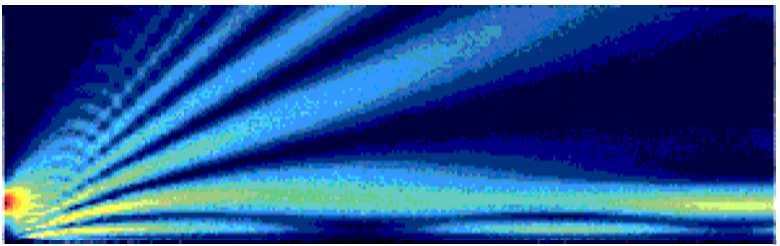
Horizontal range 2 km

Figure 2. Gaussian beam, vertically polarized, scattered from a flat surface, for a linear refractive index.



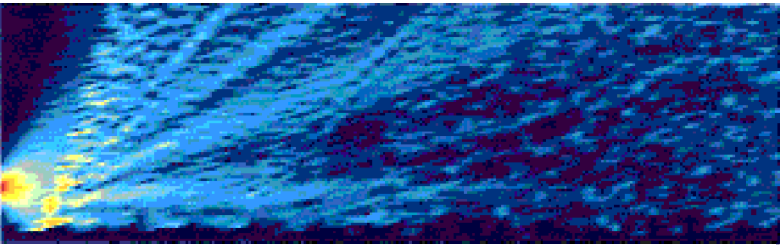
Horizontal range 2 km

Figure 3. Gaussian beam, vertically polarized, scattered from a Pierson-Moscoviz surface, for a linear refractive index.



Horizontal range 2 km

Figure 4. Gaussian beam, vertically polarized, scattered from a flat surface, for the log-linear refractive index profile given in figure 7.



Horizontal range 2 km

Figure 5. Gaussian beam, vertically polarized, scattered from a Pierson-Moscoviz surface, for the log-linear refractive index profile given in figure 7.

effect on the beam in the range of 2 km in which we present our results. A value of $1/c_1 = 0.01$, however, gives rise to significant refractive index variations (figure 7).

For a flat surface the resulting field intensity is shown in figure 4. In this case, surface scattering is far more pronounced as the profile traps the energy near the surface, where it becomes repeatedly scattered. This is shown in figure 5.

We consider now the dependence of ducting on the value of c_1 and the relative position of source and duct heights. Figure 8 shows the intensity, again for a flat surface, for the value $1/c_1 = 1.205 \pm 0.005$. Much greater ducting is apparent in comparison with figure 4. This is largely mitigated for a source even slightly higher, at 10 m, as shown in figure 9.

Finally we consider an example of the effect of random spatial fluctuations about the mean refractive index profile. (This is done in part to illustrate the flexibility of the above model.) Such variations will inevitably occur, and are due mainly to turbulent mixing of water vapour in the atmosphere, with strength and length scales in practice depending upon climate and weather. On the small spatial scales relevant to this study, the spatial spectrum correlation function of this variation might therefore be expected to obey a power-law decay. In our example a small random perturbation was added to the log-linear refractive index above. This perturbation was assumed to have scale sizes of 4 m in the vertical and 50 m horizontally, and to represent about 5% of the total refractive index. The result is given in figure 10, for a flat surface with the parameters of figure 8. Considerable scattering has resulted, partly destroying the detailed intensity pattern of figure 8.

5. Conclusions

This paper has presented a model for the treatment of a wave scattered by a rough sea surface, in the presence of ducting which may cause refraction and multiple scattering of the wave by the surface. The effect of an upwardly-refracting linear refractive index profile has first been shown. In this case the signal close to the surface is weak so that surface scattering is limited.

When the refractive index profile becomes log-linear as for the evaporation duct the situation changes. The logarithmic part of the profile, that is the part where the refractive index decreases with height, traps part of the beam close to the surface. There are high intensity directions which are trapped in the duct. Another part of the beam bends away from the surface since the refractive index starts increasing for heights greater than the duct thickness. When the surface becomes rough, the high intensity directions do not contain so much energy as in the flat surface case. Thus, the part of the beam that gets trapped in the duct is weaker and weakens further with distance due to the repeated scattering from the rough surface. As a result, the trapped part of the beam dissipates with distance. An increase in the strength of the duct results in an increase in the amount of energy that gets trapped and in the distance over which this occurs.

Attention has been restricted to the case of a vertically polarized Gaussian beam where we use the modified image medium method [1]. Results for the horizontally polarized beam, which are obtained by the image medium method in the same way, [1], show similar dependence on ducting but are less sensitive to surface roughness. This model allows the efficient numerical solution for an electromagnetic wave propagating through an irregular medium over a rough,

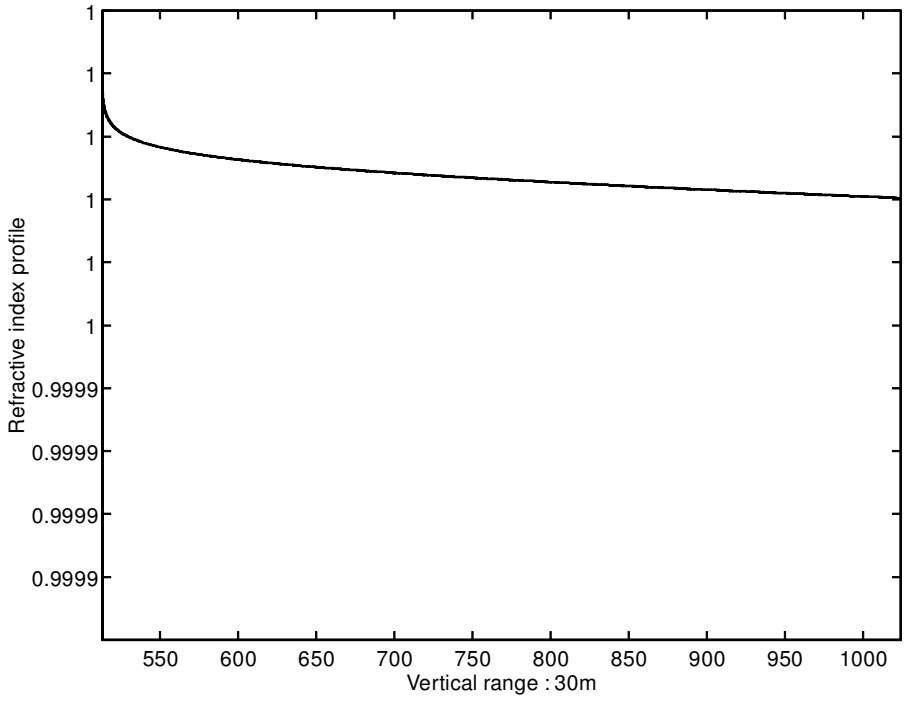


Figure 6. Log-linear refractive index profile for $1/c_1 = 1.205$.

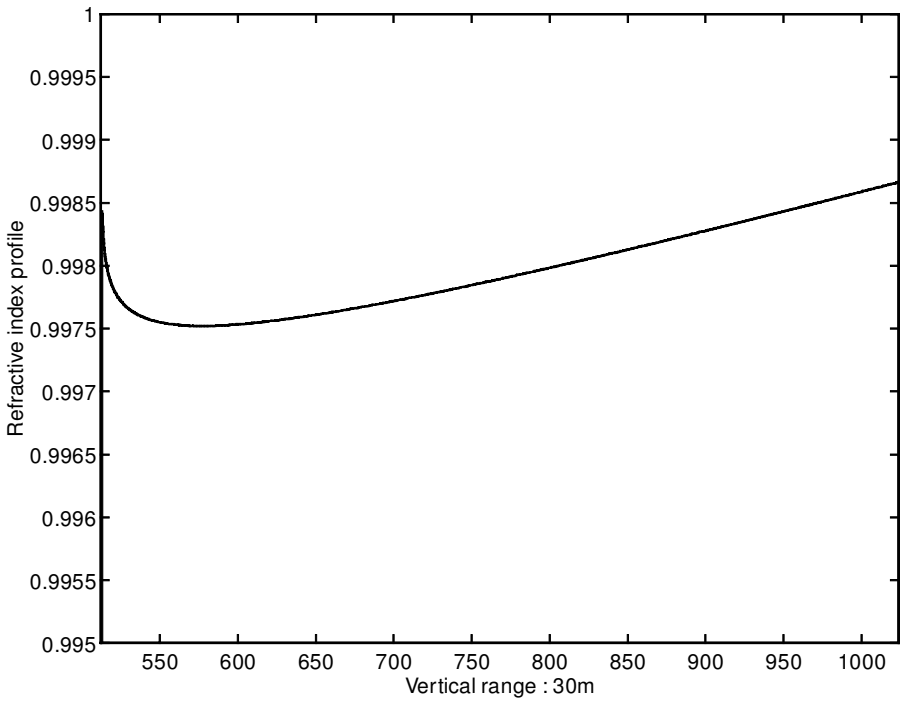
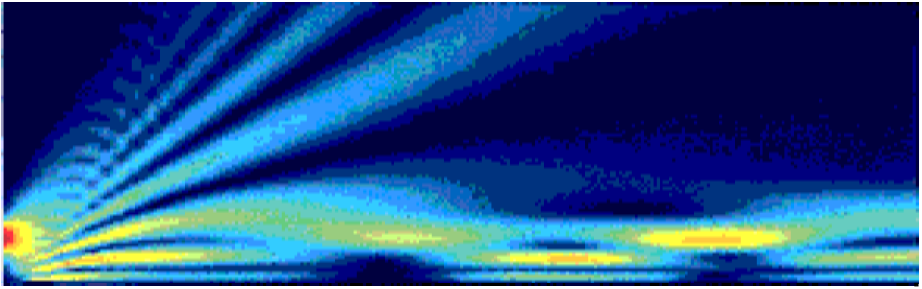
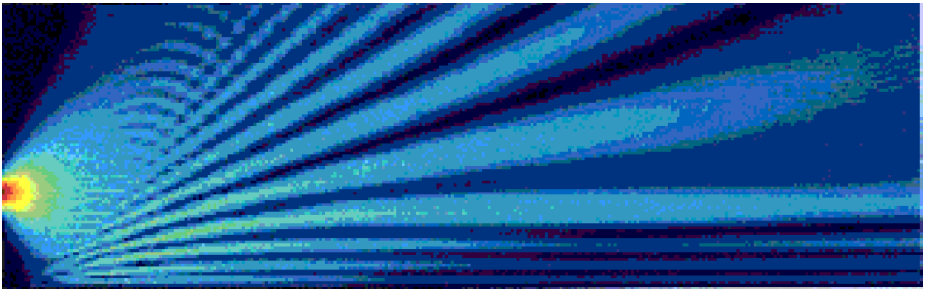


Figure 7. Log-linear refractive index profile for $a/c_1 = 0.01$.



Horizontal range 2 km

Figure 8. Gaussian beam for the log-linear refractive index profile, with parameter $1/c_1 = 0.005$.



Horizontal range 2 km

Figure 9. Intensity pattern for the parameters of figure 8, for a source at height 10 m.



Horizontal range 2 km

Figure 10. Intensity pattern for parameters of figure 8, in a medium with refractive index fluctuating randomly about the log-linear profile of figure 8.

possibly conducting, surface. Typical computation times for all cases shown here were around 2 s on a moderate workstation.

Evaporation ducts frequently occur in the refractive index profile above the sea surface due to various natural causes such as mist, cloud precipitation, wind etc. Such ducts can have a strong effect on propagation and even improve transmission.

The combination of the evaporation duct and the image medium methods described in this paper can be useful in the study of electromagnetic wave propagation over rough surfaces since, even for a constant reflection coefficient, integral equations cannot be applied in this case to a varying refractive index profile.

Acknowledgments

This work was carried out with partial financial support from the UK Ministry of Defence under a Gassiot meteorological research award (MS). YH was supported by a PhD studentship from the UK Natural Environment Research Council, and the authors are grateful to Dr B. J. Uscinski for helpful discussions and advice.

References

- [1] HATZIOANNOU, Y., 1999, *J. mod. Optics*, **46**, 35.
- [2] BROWN, G. S. (ed.), 1998, *IEEE Trans. Ant. Prop.*, **46** (special issue on low-grazing-angle backscatter from rough surfaces).
- [3] VORONOVICH, A. G., 1996, *Radio Sci.*, **31**, 1519.
- [4] BARRICK, D. E., 1995, *Radio Sci.*, **30**, 563.
- [5] KAPP, D. A., and BROWN, G. S., 1996, *IEEE Trans. Ant. Prop.*, **44**, 711.
- [6] SPIVACK, M., KEEN, A., OGILVY, J.A., and SILLENCE, C., 2000, *J. mod. Optics* (to appear).
- [7] THORSOS, E., 1987, *J. acoust. Soc. Am. Suppl. 1*, **82**, S103.
- [8] SPIVACK, M., 1995, *J. acoust. Soc. Am.*, **97**, 745.
- [9] COLLINS, M., LINGEVITCH, J. F., and SIEGMANN, W. L., 1997, *Wave Motion*, **25**, 265.
- [10] COLLINS, M., and DACOL, D.K., 2000, *J. acoust. Soc. Am.*, **107**, 1937.
- [11] USCINSKI, B. J., 1993, *J. acoust. Soc. Am.*, **94**, 491.
- [12] ROTHERAM, S., 1974, *Marconi Rev.*, **37**, 18.
- [13] JESKE, H., 1974, *Proceedings of the NATO Advanced Study Institute*, Sorrento, Italy (Holland: D. Reidel Pub. Co.), p. 130.
- [14] BEAN, B. R., and DUTTON, E. J., 1966, *NBS Monograph*, **92**.
- [15] MONIN, A. C., and OBUKHOV, A. M., 1954, *USSR Acad. Sci. Geophys. Inst.*, **24**, 163.
- [16] THORSOS, E. I., 1990, *J. acoust. Soc. Am.*, **88**, 335.